AIMS Energy, 11(3): 522–539.
DOI: 10.3934/energy.2023027
Received: 22 January 2023
Revised: 17 May 2023
Accepted: 18 May 2023
Published: 08 June 2023

http://www.aimspress.com/journal/energy

Research article

Experimental evaluation of a solar water heater integrated with a corrugated absorber plate and insulated flat reflectors

Nassir D. Mokhlif[1,*], Muhammad Asmail Eleiwi[2,3] and Tadahmun A. Yassen[2]

[1] Department of Petroleum and Gas Refining Engineering, College of Petroleum Processes Engineering, Tikrit University, Tikrit, Iraq
[2] Department of Mechanical Engineering, College of Engineering., Tikrit University, Tikrit, Iraq
[3] Department of Electromechanical Engineering, College of Engineering., University of Samarra, Samarra, Iraq

* **Correspondence:** Email: nassirdhamin@tu.edu.iq; Tel: +9647715532938.

Abstract: When it comes to renewable energy, solar water heaters are among the fastest-growing technologies. Comparatively speaking, integrated collector-storage solar water heater systems cost less than other solar water heater designs. Therefore, both the construction and the operation of a combined collector-storage solar water heater are quite straightforward. The integrated storage solar collector coupled with reflectors has been experimentally investigated. The reflectors were insulated from the back side when working during the day hours and as insulated cover during the night hours. While comparing the combined collector-storage solar water heater with and without insulated reflectors, the results showed that the insulated reflectors increased the thermal efficiency by 23%. Furthermore, on the coldest day, the stored water reached a high of 82 degrees Celsius, though it was only 46 degrees Celsius that same morning.

Keywords: integrated solar water heater; reflectors; corrugated absorber; double glass

1. Introduction

Energy is the mainstay of human actions and has a crucial significance in economical evolution as there's a vigorous relationship between the economical action and the energy. In history, fossil fuel in its solid state, such as coal and wood, has been a major energy source. Additionally, an increase in

the worldwide energy needs owing to the growth of population and 20th century manufacturing development drives the fossil fuel throughout a transitional state. It's broadly realized that, for a maintainable evolution, currently utilized energy means, such as fossil fuel and nuclear power, must be rapidly substituted via the sources of renewable energy, the latter being maintainable and possesses the prospective for meeting current and forthcoming needs of projected global energy without causing any ecological influences [1]. The sources of renewable energy, like hydropower, wind, biogas, and solar, are prospective nominees for meeting the worldwide requests of energy in a maintainable manner. Solar water heaters (SWH) are the quickest rising technology in the sector of renewable energy. The majority of the designs of SWHs can be categorized into (3) sets: forced circulation, natural convection, and integrated collector storage (ICS) with SWH. Additionally, the setting of ICS-SWH is relatively easy in design as well as operation, with the costs of the systems of ICS-SWH being relatively less than those for other designs of SWHs [2]. In these systems, the collection of solar energy and the storage of hot water takes place in a sole unit. Additionally, the system of ICS-SWH works as an isolated one without moving components and permits the operator to be grid electricity independent. Owing to the big thermal mass that is linked with the surface of absorber, such water heaters possess an intrinsic capability for avoiding freezing in numerous circumstances. The systems of ICS-SWH need a slight upkeep, other than the glazing surface's periodic cleaning, as well as possess the capability for providing the hot water steadily and dependably for several years. Kumar and Prakash [3] experimentally and numerically investigated the efficiency enhancement of an ICS-SWH. This improvement is presented via the Vee-corrugation of an absorber and the design optimization for the Vie-included angle throughout the simulation, as well as through investigational work. The 8-corrugation model's efficacy was found to be better than the 5-corrugation model for similar ambient circumstances. Additionally, it was hypothetically inferred that the optimized regime includes the 18-corrugation model and a 28.78° Vie-included angle. Mokhlif [4] experimentally studied an ICS-SWH system with a corrugated absorber plate, as well as a dual glazing cover. The influence of the dual glazing cover upon the ICS-SWH performance was investigated. Dual-glazing cover situations were found to have storage water temperatures that were 6 and 11 degrees Celsius higher than those of single-glazing cover situations on the first morning of the second and third days, respectively. The mean daily thermal efficacy of built regime was 68% with a 0.0091 kg/s rate of mass flow. The daily thermal efficacy in the dual-glazing cover situation was higher than that of the single-glazing cover situation by 4.6%. Yassen [5] experimentally investigated an ICS-SWH system with a corrugated absorber plate and a single glazing cover. The ultimate temperature of stored water was 59 ℃ during the coldest day in January for the environment of Iraq. It was found that the obtained temperature of the stored water was more than for the preceding investigation, mainly attributed to the storage tank's corrugated absorber. Taheri [6] experimentally studied an ICS-SWH system with a flat plate absorber as well as a dual-glazing cover. The heating regime consisted of sands having a black color and was submerged into a storage tank of water that built the chief portion of the absorber unit of collector absorber. In terms of the whole outcomes of the experiments, the average day-to-day efficacies of the collector performed more than 70%. Additionally, the obtained outcomes obtained revealed that the topmost temperature value of stored water the tank obtained was around 52 ℃. Barone [7] investigated a prototype of an elevated-vacuum ICS-SWH. The suggested unit reached the elevated stored water temperatures as well as reduced a drop of temperature during non-collection times. Such objective was conducted via the suppression of the losses of convective heat into the regime by maintaining the pressure into the connected enclosure less than 0.01 Pa and by implementing a particular choosy

coating to the absorber surface of the solar to extremely decrease the radiative losses. Bilardo [8] studied a novel solar integral collector storage (ICS) to produce domestic hot water (DHW). The originality comprised of joining a surface of absorbent material, a storage cavity produced from a phase change material (PCM), and heat pipes in a sole dense covering. Additionally, the energy achievement of the system was experimentally investigated in a variety of seasons during the year, with and without the manufacture of the domestic hot water. During the investigational stage, the thermal storage obtained an ultimate temperature of 79.3 ℃, developing the latent heat of PCMs. The general achievements manifested a virtuous covenant, with outcomes obtainable in the literature regarding the energy storage and efficiency. Harmim [9] investigated a novel (ICS-SWH) attached with a linear parabolic reflector. An apparatus was designed to integrate a facade of construction in the Algerian Sahara for meeting the households' hot water requirements during the winter season. The equipment numerical model was evolved and a prototype was built and experimentally tested. The investigational tests evinced that the apparatus was merely active through the wintertime. Its average daily efficiency varies from 36.4% to 51.6%, and its thermal losses coefficient varies from 2.17 $W.K^{-1}$ to 3.12 $W.K^{-1}$ throughout the night. Beneath the bright sky at a primary temperature of 22 ℃, the temperature of water reaching a peak at (49 ℃). Rao and Somwanshi [10] presented a general summary regarding the systems of compact ICS-SWH, which can be beneficial for an additional investigation for designing and developing a fresh small size SWH. Sadeghi [11] studied the solar water heater with a phase change material (PCM) to absorb and release heat during day and night continuously, from the working fluid. This solar collector-storage system was shown to increase thermal efficiency in the stagnation mode from 66% to 82%. Mahmoudi [12] contributed a design of solar water heater coupled with an inorganic material (sodium acetate trihydrate) as a PCM for storage heat, as it has a higher storage heat capacity compared to the organic materials.

Highly famous systems of SWH employed being a one of a kind thermo-siphon, which is comprised of a solar collector having channels that are bounded either upon or throughout the plate of absorber, in addition to a storage tank. Such composite systems met many problems, such as leaks throughout the joins, and the corrosion produces an unavoidable heat energy loss resulting in a reduction in efficacy. Additionally, the parts multi-plexing augmented the cost of upkeep in such regimes. Therefore, numerous investigators attempted to utilize an ICS-SWH system which integrates the solar collector and the storage tank in a sole section. Such regimes decrease the welded joints as well as the linked components' bends. Thus, the present study concentrated on enhancing the ICS-SWH performance. The whole of the ICS-SWH preceding investigator's research were performed by using the insulated cover to reduce the heat losses through the hours of night. In the current work, the insulated cover was improved by adding a mirror to the front side to act as a reflector during the day hours. Therefore, the cover will have a multiple functions, which reduces heat losses during the night and reflects during the day. The reflector will increase the solar intensity falling on the plate of absorber, thereby leading to an increase the stored water temperature. Thus, the current work aims to experimentally investigate the achievement of ICS-SWHs coupled with a reflector-insulator cover.

2. Method and material

The details of the regime evolved methodology are clarified into the present section in relation to the details of the constructed system, the experimental setup, the measuring instruments, and the proceeding of measurements, as well as the periodic thermal efficacy.

2.1. Details of system construction

The schematic diagram of the suggested ICS-SWH is elucidated in Figure 1. It is comprised of a storage tank (ST) having an insulated box, a top corrugated absorber, and two glazed panels' covers. Additionally, a solar collector has been designed as a corrugated ST with a triangular shape. Dimensions, including width (W_c) and depth (D_c) for the absorber plate's five triangular corrugations, have been similarly designed to be 0.2 m in width and 0.1 in depth. The space between the tank's bottom and baseline beneath the corrugation is around 2 cm. Therefore, the entire depth (D_{st}) of the ST is 0.12 m. The tank's-built plates were prepared from galvanized steel, with a thickness of 2 mm. The eventual dimensions, including the length, width, and depth, of the entire ST were 1, 1, 0.12 m, respectively. According to these parameters, the ST carrying capacity would be 70 L. For increasing the thermal absorption, a dye having a dark black color was utilized for painting the ST's undulating external surface. In addition, a layer of glass wool insulation 0.1 m thick covers the entire tank, except the top, to reduce heat loss. The tank's top corrugated side was left open, exposing an air gap on the other side. Eventually**,** the entire ST and the insulation was positioned in a structure prepared from a square un-galvanized steel channel that was covered by galvanized sheets with a 0.8 mm thickness. In addition, the overall measurements of the frame box were as follows: 1.2, 1.2, and 0.27 m. The frame top was prepared from a dual–glazing cover with a thickness of 4 mm. The glaze (S_{dg}) layers were gapped with 5 cm of air. Two reflectors were fixed on the upper and lower sides. The inclination angle (θ) of the reflectors was 60° to the inclination of the collector. The inclination angle of the selected reflectors were adjusted to capture a maximum solar intensity at the peak. Every reflector has a length (L_R) of 0.5 m. The reflectors were insulated from the back side with a 2 cm layer of cork to work as a cover during the night for reducing the loss of heat from the collector's top side. Therefore, the reflector works during the day to raise the solar radiation intensity that falls upon the collector. In addition, the reflector works as an insulation cover during the night to reduce the heat losses from the top side of the collector. The whole water heater being fixed at a 40° inclination angle from horizon, as well as focused on the South. Table 1 lists the design factors in addition to their magnitudes for the present heating system.

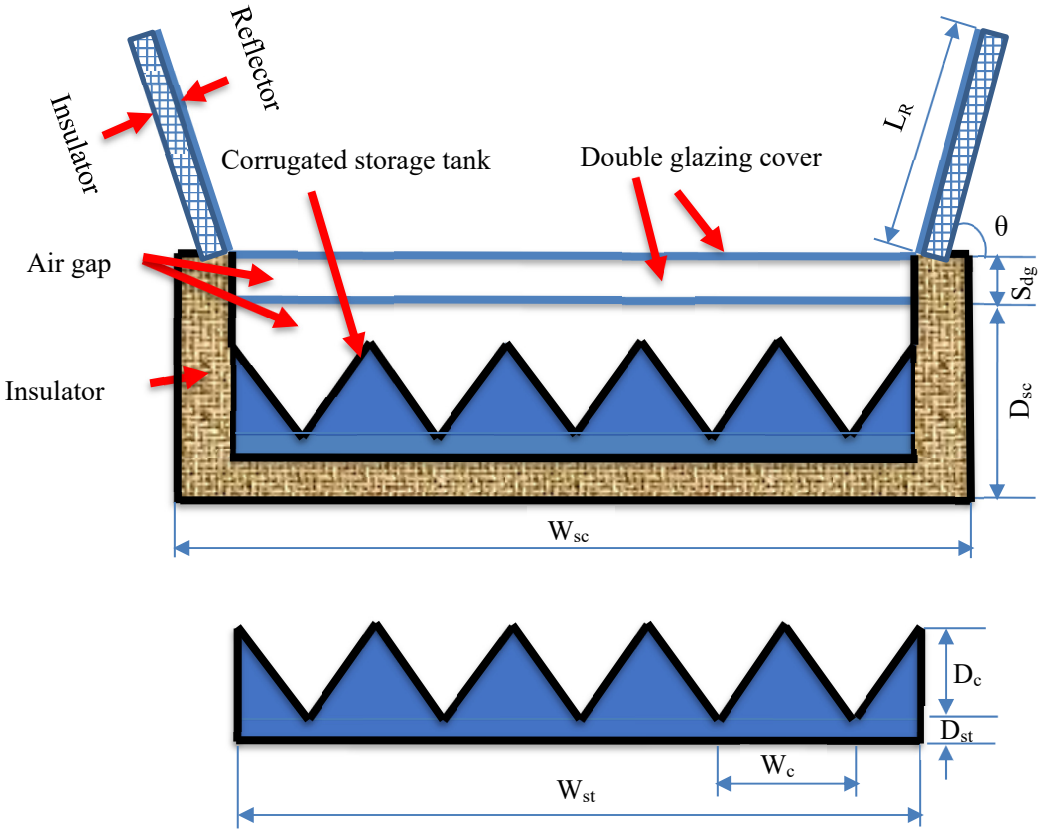

Figure 1. Design of the ICS-SWH coupled with reflector-insulator cover.

Table 1. The design factors of SWH.

Collector	**ICS-SWH**
Aperture area (A)	1 m^2
Depth (D_{sc})	0.27 m
Inclination angle (β)	40°
Length (L_{sc})	1.2 m
Width (W_{sc})	1.2 m
Reflector	**Mirror**
Back insulation thickness	2 cm
Inclination angle (θ)	60°
Insulation type	cork
Length (L_R)	0.5 m
Number	2
Storage Tank	**Corrugated**
Absorber emissivity (ε_p)	0.9
Absorber type	non-selective
Material	Galvanized steel gage 2 mm
Corrugation depth (D_c)	0.1 m
Corrugation width (W_c)	0.2 m
Storage tank depth (D_{st})	0.12 m
Storage tank length (L)	1 m
Storage tank width (W_{st})	1 m
Paint	Black
Transparent Cover	**Glass**
Glazing space (S_{dg})	5 cm
Number	Double Layer
Thickness	4 mm
Insulation	**Glass wool**
Thickness	0.1 m

2.2. The setup experiments and the measuring instruments

For measuring the temperature change within the evolved regime, six calibrated kind (K) thermocouples (Chromel-Alumel) with a range of 50–1000 ℃ and an accuracy of ±0.1) have been utilized, as revealed in Figure 2. The 1st thermocouple has been fixed at the water inlet tube for measuring the temperature of discharged water. The 2nd thermocouple has been fitted at the outlet pipe of tank for measuring the departing water temperature. The 3rd, 4th, and 5th thermocouples were set in the ST for measuring the temperature change within. Finally, the 6th thermocouple was utilized to measure the outside temperature. All thermocouples were connected to a data logger type Applent AT4808. In addition, an accurate Sun Digital Meter (Daystar DS-05A) was used to measure the irradiation, with an accuracy of ±3%. In this research, the volumetric flow rate of the water was manually measured by collecting a known water volume vs time.

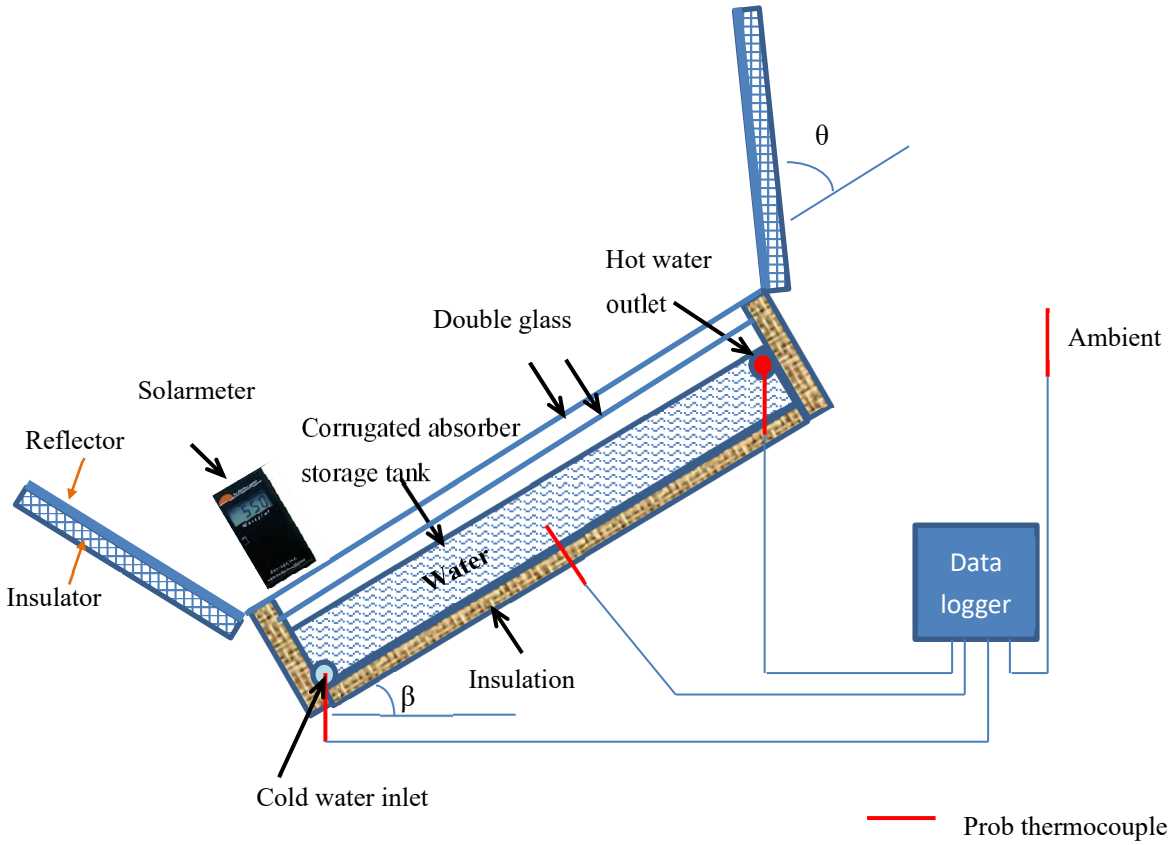

Figure 2. Schematic diagram of the investigational setup.

2.3. The proceeding of measurements

A group of regular-experimental attempts has been performed via the team of research for evaluating the achievement of the system of synthesized SWH with a dual glazing cover and the back insulated reflectors**,** displayed in the Figure 3, at the University of Tikrit in Iraq. The tests were conducted on the assumption that the solar radiation, wind speed, and water temperature would remain constant throughout the course of one hour.

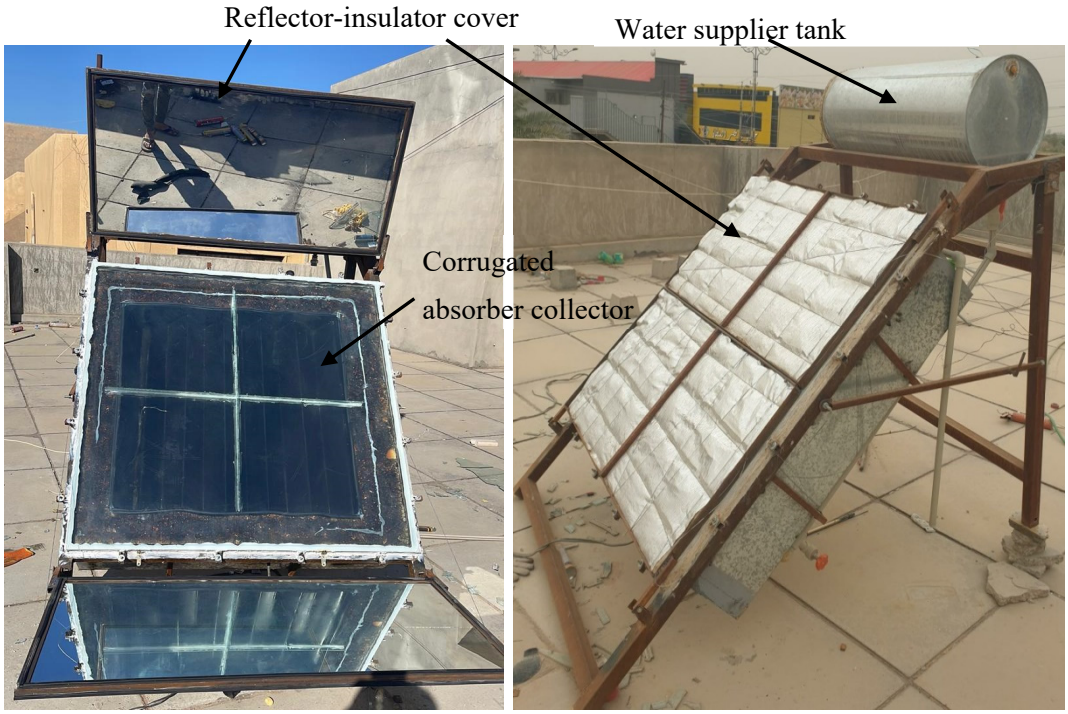

Figure 3. Test rig of the present ICS-SWH.

2.4. Overall thermal efficiency

The heat input to the SWH is [13,14]:

$$Q_{in} = \int_0^t IA\, dt \tag{1}$$

where:

t (s): Collection time of the solar radiation through a day,

I: Global solar radiation in W/m^2.

Additionally, the heat outlet from the SWH is [14–17]:

$$Q_{out} = \int_0^{t_1} \dot{m} C_w (T_{out} - T_{in}) dt \tag{2}$$

where:

$\dot{m}$: The mass flow rate of water that drained from the SWH,

C_w: The heat capacity of water in kJ/kg.^{o}C.

Additionally, the heat that stored inside the SWH beyond the sunset is [18]:

$$Q_{stor} = m_w C_w \left(T_{wf} - T_{a-1}\right) \tag{3}$$

The average thermal efficiency for one day with the incorporated SWH load can be stated as [19]:

$$\eta_{wl} = \frac{Q_{stor} + Q_{out}}{Q_{in}} \tag{4}$$

Substituting Eqs (1–3) into Eq (4) can be used for calculating the average daily thermal efficacy of a thermal regime by the subsequent formula:

$$\eta_{wl} = \frac{m_w C_w (T_{wf} - T_{a-1}) + \int_0^{t_1} \dot{m} C_w (T_{out} - T_{in}) dt}{\int_0^t IA dt} \quad (5)$$

Where the average temperatures of water were stated via $T_{a\text{-}1}$ & T_{wf} representing the heating process suppliant and the withdrawal final period of time, respectively, and t_1 and m_w are the water withdrawal time from the SWH (not comprising the final withdrawal of water) and the water mass of ST, respectively. The advantageous quantity of heat generated via the SWH is stated via Eq (5), with the equation's denominator being the solar radiation hitting above the glass cover per the matching time period.

Efficacy of the system is computed via the following formula (the load isn't comprised in this formula):

$$\eta_{wol} = \frac{Q_{stor}}{Q_{in}} = \frac{m_w C_w (T_{wf} - T_{a-1})}{\int_0^t IA dt} \quad (6)$$

3. Results and discussion

3.1. Performance of ICS-SWH without reflector and load

Study of the SWH performance and the stored water temperature for one day was required. Therefore, through 26th January of 2022, the regime was examined without load for one day, initiated from the first day's sunrise to the following day's sunrise. The data for the experiment was collected on the coldest day of the year in Tikrit. The time-dependent variations in solar radiation, bottom-stored water temperature, top-stored water temperature, and ambient temperature are shown in Figure 4. In the end, the experiment produced solar radiation of 1150 W/m^2 at 1:00 P.M. The highest ambient temperature measured during the experiment was 12 degrees Celsius at 3:00 P.M. Additionally, the least logged ambient temperature through the experiment was –3 ℃ at 7:00 A.M. the following morning. The tank's stored water was heated from the lowest temperature of 10 ℃ to the ultimate temperature of 69 ℃. The ultimate temperature of the stored water rose by the day period until reaching the ultimate of 69 ℃ at 3:30 P.M. It stayed at 69 ℃ from 3:30 P.M. until 4:30 P.M. The stored water's temperature gradually dropped from there, reaching a low of 38 ℃ the next morning, at 7:00 AM. This is because, up until 4:30 P.M., the absorber was the only thing keeping the water in the tank warm; following this, the water warmed the tank, which warmed the surrounding air. The water's temperature dropped from 63 ℃ overnight to 38 ℃. The water's temperature dropped to 15 ℃ overnight. The results of the ICS-SWH tested by Mohsen [20] manifested that the temperature of the stored water reduced more than 20 ℃ during the whole night. Kumar and Rosen [3] evinced that temperature of the stored water decreased to about 15 ℃ through the entire night. That means that the present ICS-SWH performed well due to improved insulation and sealing.

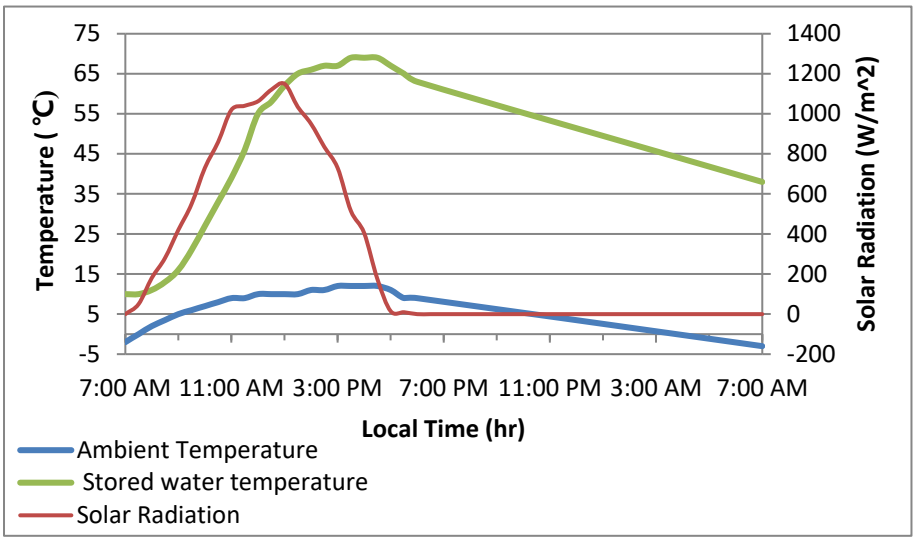

Figure 4. Temperature change of the stored water with the local time on 26th January of 2022.

3.2. Performance of ICS-SWH with reflector-insulator cover and without load

Figure 5 elucidates the variables of environmental conditions, which are the air temperature and solar radiation, as well as the change in the water tank temperature. Additionally, the experiment was carried out with two reflectors and without any load during the clear and sunny day of January 31, 2022. The highest air temperature was 16.3 ℃ at 3:00 P.M. in the afternoon. The lowest ambient temperature was 2 ℃. The ultimate solar radiation value was 1303 W/m^2 in the afternoon. At about 3:30 in the afternoon, the tank's hot water reached its peak temperature of 82 ℃. The combination of direct solar energy from the sun and solar radiation reflected by the reflectors produced the greatest stored water temperature. Then, the temperature of the stored water started to drop until reaching the lowest value of 46 ℃ at 7:00 A.M. following morning. Additionally, the high stored water temperature remained until the next morning because the reflectors covered the top of the ICS-SWH and worked as an insulator. The temperature of the water in the tank was increased from 14 ℃ to 82 ℃. It implies that between 7 A.M. and 3:30 P.M., the water in storage tanks heated up by 68 ℃.

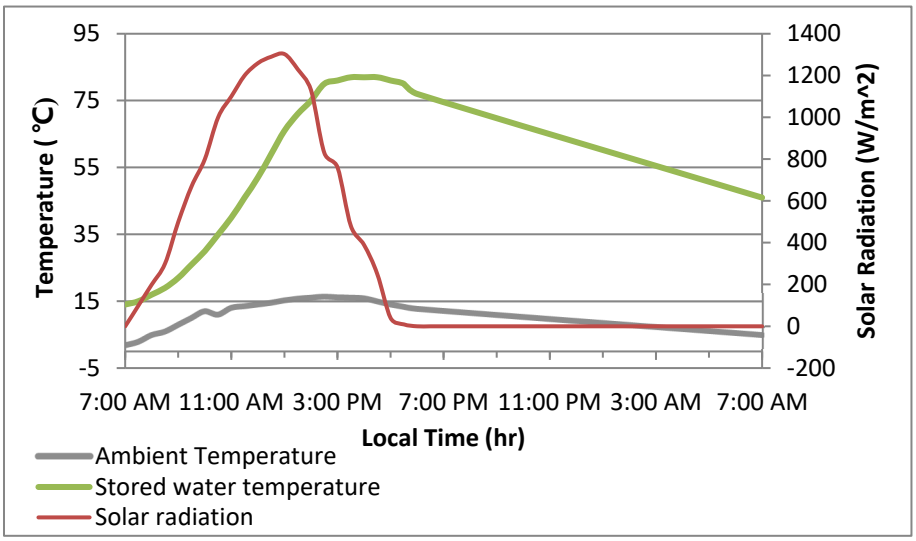

Figure 5. The time zone shifts of the water's temperature on January 31, 2022.

Table 2 portrays the comparison between the current work and the preceding works in term of the maximum rise in temperature of stored water. It can be noted that for the previous works, the maximum rise in the stored water temperature obtained by Yassen [5] was 58 ℃. For the present ICS-SWH, without and with reflectors, the maximum rise in the stored water temperature during the coldest month (January) is 69 ℃. That means the present ICS-SWH for the present work without reflectors performed better than the ICS-SWH for the previous works. This is because the reflectors increase the solar radiation intensity upon the plate absorber and increases the temperature of stored water. This increase in temperature of the stored water is very convenient for domestic use.

Table 2. Comparison between the current work and the preceding works in term of maximum rise in the stored water temperature.

Reference	Maximum solar radiation (W/m^2)	Ambient temperature range (℃)	Maximum rise in stored water temperature
[3]	750	(15)–(25)	65
[20]	1000	(0)–(15)	55
[21]	1100	(25)–(35)	65
[5]	930	(5)–(17)	58
Present ICS-SWH without reflectors	1150	(–3)–(12)	69
Present ICS-SWH with reflectors	1303	(3)–(16.3)	82

3.3. Performance of ICS-SWH with reflectors and load

Figure 6 demonstrates the variation of environmental conditions, which are the ambient temperature and the solar radiation intensity. This figure manifests the temperature variation of the stored water. The experiment was carried out for the ICS-SWH coupled with two reflectors and the test was achieved with a load of 0.0025 L/s (9 L/hr.) on 6th February of 2022. Around 3 o'clock in the afternoon, the temperature was at its greatest (17.8 ℃), and at 7 o'clock in the morning, it was at its lowest (5 ℃). At 3:30 in the afternoon, the output hot water temperature reached a maximum of 76 ℃,

and the maximum solar radiation value was 1320 watts per square meter at 1:00 in the afternoon. Additionally, the ICS-SWH had water entering it at a temperature of 22 ℃ at 3:30 P.M. Moreover, the ICS-maximum SWH's inlet-to-outlet temperature difference was 54 ℃ at 3:30 P.M. With a mean temperature of 69 ℃, the 54 liters of hot water produced by the ICS-SWH throughout the burden period, beginning at 12:00 noon and ending at 6:00 P.M. At 6:00 P.M., the remaining water volume in the tank was 70 liters and the temperature was 65 ℃. It implies the ICS-SWH was able to obtain 124 liters of water up to a comfortable household temperature of 67 ℃ for usage during the winter.

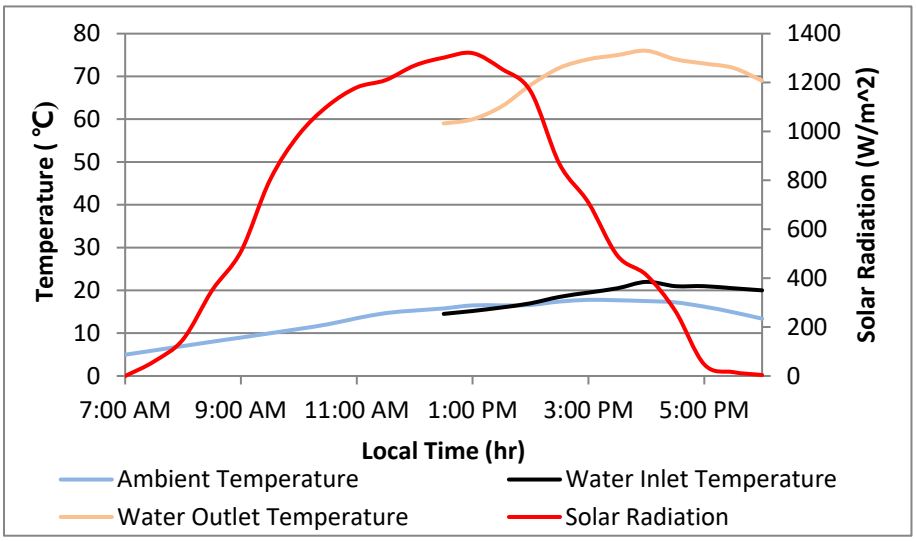

Figure 6. The time zone shifts of the water's temperature on February 6, 2022.

Figure 7 reveals the variation of environmental conditions, which are the ambient temperature, solar radiation intensity, and the stored water temperature. The experiment was performed on a ICS-SWH coupled with two reflectors. The test was achieved with a 0.00491 $kg.s^{-1}$ (17.7 $L.hr^{-1}$) load on 8th February of 2022. Air temperatures ranged from a high of 18 ℃ at 3:00 P.M. to a low of 5 ℃ at 7:00 A.M. The highest amount of solar radiation was measured to be 1331 W/m^2 at 1:00 P.M. At 3:30 P.M., the water entering the ICS-SWH was 20 ℃, while the exit hot water temperature reached a maximum of 68 ℃. Moreover, the maximum temperature difference between the ICS-input SWH's and exit was 48 ℃ at 3:30 P.M. The ICS-SWH provided 106 liters of hot water at an average temperature of 61.6 ℃ from the start of the burden period (12 PM) to the end of the day (6 PM). The amount of water remaining inside the tank after 6:00 P.M. was 70 liters at a temperature of 48 ℃. That means the ICS-SWH heated 176 liters of water at a temperature of 56 ℃, which is suitable for domestic use during the winter season.

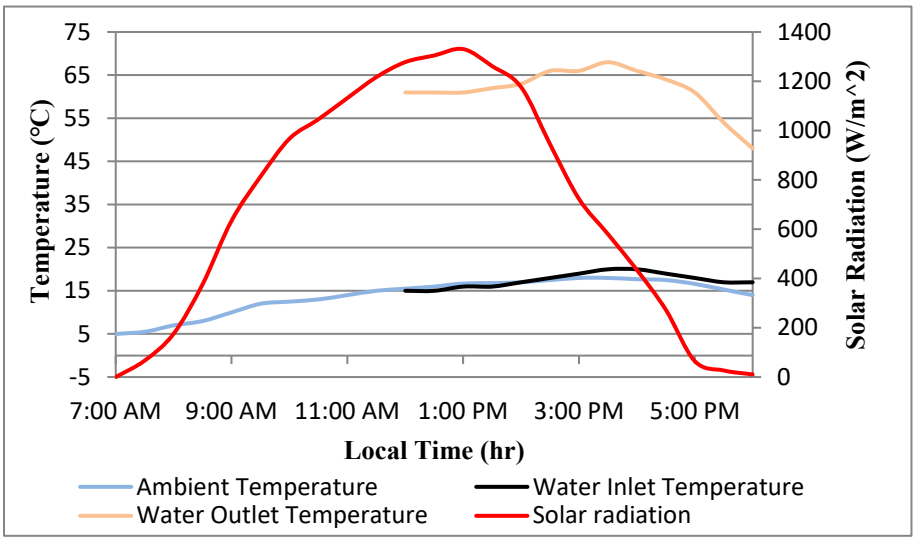

Figure 7. The time zone shifts of the water's temperature on February 8, 2022.

3.4. Daily thermal efficacy

The calculated values of daily thermal efficacy for the present ICS-SWH are listed in Table 3. The mass flow rate of water was 0.0025 kg.s^{-1} and the heat amount entering the ISWH due to solar radiation was 27.8 MJ during the day. The amount of heat carried out due to the flow rate of the water outlet from the ICS-SWH was 10.5 MJ. As for the residual heat stored in the tank at the end of the day, it was 9.8 MJ, and thus, the average daily thermal efficacy was 73%. At the mass flow rate of 0.00491 kg.s^{-1}, the heat input quantity to the ICS-SWH obtained from the solar radiation was 28.5 MJ. Exhausted water from the regime carried 18.2 MJ of energy, while the remaining water in the tank transported (calculated at sunset) an additional 7.1 MJ. This means that on a daily basis, the thermal efficiency was 88.7%.

Table 3. Energy balance and daily average thermal efficiency of a SWH at three different flow rates.

Flow rate (Kg/s)	Inlet heat (MJ)	Outlet heat (MJ)	Storage heat (MJ)	Mean daily thermal efficiency (%)
0.0025	27.8	10.5	9.8	73
0.00491	28.5	18.2	7.1	88.7

3.5. Results validation

The current investigation has been confirmed via the comparison of the obtained outcomes from the investigational preceding studies with the outcomes of present work, as manifested in Table 4. Yassin [5] determined that the total daily thermal efficacy was 59% when the storage tank volume, glazing cover, and mass flow rate were 140 liters, single, and 0.005 kg/s, respectively. Mokhlif [4] found that the total daily thermal efficacy was 65% when the storage tank volume, glazing cover, and mass flow rate were 140 liters, double, and 0.00916 kg/s, respectively. For the present work (ICS-SWH with reflector-insulator cover), the total daily thermal efficacy was 73% when the storage tank volume, glazing cover, and mass flow rate were 70 liters, double, and 0.0025 kg/s, respectively. For the present

work (ICS-SWH with reflector-insulator cover), the total daily thermal efficiency was 88.7%when the storage tank volume, glazing cover, and mass flow rate were 70 liters, double, and 0.00458 kg/s, respectively. It can be noted that the thermal efficacy for the current investigation was higher compared to the preceding works because of the insulating reflectors. The insulating reflector works during the day to reflect the solar radiation to the absorber plate and increases the water stored temperature. Additionally, the insulating reflector works during the night as an insulator and reduces the heat losses by covering the top side of the ICS-SWH.

Table 4. The daily thermal efficacy's comparison of present work with previous works.

Reference	Flow rate (kg/s)	Tank size (L)	Glassing cover	Inlet heat (MJ)	Outlet heat (MJ)	Storage heat (MJ)	Mean daily thermal efficiency (%)
[5]	0.005	140	Single	46.6	16.2	11.2	59
[5]	0.00916	140	Single	41.8	20.3	6.7	65
[4]	0.00916	140	Double	39	20.7	5.9	68
Present work	0.0025	70	Double	27.8	10.5	9.8	73
Present work	0.00458	70	Double	28.5	18.2	7.1	88.7

4. Conclusions

The ICS-SWH coupled with insulated reflector cover was experimentally investigated. The reflectors were insulated from the back side for working as reflectors during the day hours and as an insulated cover during the night hours, which increases the solar intensity that reaches the collector during the day and reduces heat losses during the night. The results elucidated that the thermal efficacy of the ICS-SWH with insulated reflectors was enhanced by 23% compared with the ICS-SWH without insulated reflectors. In addition, the maximum temperature of stored water reaches 82 ℃ throughout the coldest day and 46 ℃ in the early morning of the coldest day. The present ICS-SWH heated 176 liters of water at the average temperature of 56 ℃, which is suitable for the domestic use during the winter season.

Use of AI tools declaration

The authors declare they have not used Artificial Intelligence (AI) tools in the creation of this article.

Conflict of interest

No potential conflict of interest was reported by the authors.

References

1. Oyedepo SO (2012) Energy and sustainable development in Nigeria: the way forward. *Energy Sustainability Soc* 2: 1–17. https://doi.org/10.1186/2192-0567-2-15
2. Kalogirou S (1997) Design, construction, performance evaluation and economic analysis of an integrated collector storage system. *Renewable Energy* 12: 179–192. https://doi.org/10.1016/S0960-1481(97)00029-3
3. Kumar R, Rosen MA (2010) Thermal performance of integrated collector storage solar water heater with corrugated absorber surface. *Appl Thermal Eng* 30: 1764–1768. https://doi.org/10.1016/j.applthermaleng.2010.04.007
4. Mokhlif ND, Eleiwi MA, Yassen TA (2021) Experimental investigation of a double glazing integrated solar water heater with corrugated absorber surface. *Mater Today Proc* 42: 2742–2748. https://doi.org/10.1016/j.matpr.2020.12.714
5. Yassen TA, Mokhlif ND, Eleiwi MA (2019) Performance investigation of an integrated solar water heater with corrugated absorber surface for domestic use. *Renewable Energy* 138: 852–860. https://doi.org/10.1016/j.renene.2019.01.114
6. Taheri Y, Ziapour BM, Alimardani K (2013) Study of an efficient compact solar water heater. *Energy Convers Manage* 70: 187–193. https://doi.org/10.1016/j.enconman.2013.02.014
7. Baronea PG, Buonomano A, Palmieri V, et al. (2022) A prototypal high-vacuum integrated collector storage solar water heater: Experimentation, design, and optimization through a new in-house 3D dynamic simulation model. *Energy* 238: 122065. https://doi.org/10.1016/j.energy.2021.122065
8. Bilardo M, Fraisse Pailha GM, Fabrizio E (2020) Design and experimental analysis of an Integral Collector Storage (ICS) prototype for DHW production. *Appl Energy* 259: 114104. https://doi.org/10.1016/j.apenergy.2019.114104.
9. Harmim A, Boukar M, Amar M, et al. (2019) Simulation and experimentation of an integrated collector storage solar water heater designed for integration into building façade. *Energy* 166: 59–71. https://doi.org/10.1016/j.energy.2018.10.069
10. Rao Anupam AS (2022) A comprehensive review on integrated collector-storage solar water heaters. *Mater Today Proc* 36: 15–26. https://doi.org/10.1016/j.matpr.2021.12.424
11. Sadeghi G, Mehrali M, Shahi M, et al. (2022) Experimental analysis of Shape-Stabilized PCM applied to a Direct-Absorption evacuated tube solar collector exploiting sodium acetate trihydrate and graphite. *Energy Conver Manage* 269: 116176. https://doi.org/10.1016/j.enconman.2022.116176
12. Mahmoudi A, Mehrali M, Sadeghi G, et al. (2022) Innovative direct solar receiver-storage systems for heat production. *Inno-DSS* Available from: https://projecten.topsectorenergie.nl/storage/app/uploads/public/623/da4/f91/623da4f91a5b5003604684.pdf.
13. Ahmadkhani A, Sadeghi G, Safarzadeh H (2021) An in depth evaluation of matrix, external upstream and downstream recycles on a double pass flat plate solar air heater efficacy. *Thermal Sci Eng Progress* 21: 100789. https://doi.org/10.1016/j.tsep.2020.100789
14. Mohammed MF, Eleiwi MA, Kamil KT (2020) Experimental investigation of thermal performance of improvement a solar air heater with metallic fiber. *Energy Sources, Part A Recover Util Environ Eff* 43: 2319–2338. https://doi.org/10.1080/15567036.2020.1833110

15. Eleiwi MA, Mohammed MF, Kamil KT (2022) Experimental analysis of thermal performance of a solar air heater with a flat plate and metallic fiber. *J Eng Sci Technol* 17: 2049–2066. Available from: https://jestec.taylors.edu.my/Vol%2017%20Issue%203%20June%202022/17_3_32.pdf.
16. Talib SM, Rashid FL, Eleiwi MA (2021) The effect of air injection in a shell and tube heat exchanger. *J Mech Eng Res Dev* 44: 305–317. Available from: https://jmerd.net/Paper/Vol.44,No.5(2021)/305-317.pd.
17. Eleiwi MA, Shallal HS (2020) Thermal performance of solar air heater integrated with air-water heat exchanger assigned for ambient conditions in Iraq. *Int J Ambient Energy* 0750: 1–22. https://doi.org/10.1080/01430750.2020.1722745
18. Eleiwi MA, Mokhlif ND, Saleh HF (2023) Improving the performance of the thermal energy storage of the solar water heater by using porous medium and phase change material. *Energy Sour Part A: Recovery Utilization Environ Effects* 45: 2013–2026. https://doi.org/10.1080/15567036.2023.2185316
19. Khalaf AE, Eleiwi MA, Yassen TA (2023) Enhancing the overall performance of the hybrid solar photovoltaic collector by open water cycle jet-cooling. *Renewable Energy* 208: 492–503. https://doi.org/10.1016/j.renene.2023.02.122
20. Mohsen MS, Al-Ghandoor A, Al-Hinti I (2009) Thermal analysis of compact solar water heater under local climatic conditions. *Int Commun Heat Mass Transfer* 36: 962–968. https://doi.org/10.1016/j.icheatmasstransfer.2009.06.019
21. Sopian K, Syahri M, Abdullah S, et al. (2004) Performance of a non-metallic unglazed solar water heater with integrated storage system. *Renewable Energy* 29: 1421–1430. https://doi.org/10.1016/j.renene.2004.01.002
22. Figliola RS, Beasley D (2015) Theory and design for mechanical measurements. *John Wiley Sons* Available from: https://books.google.iq/books/about/Theory_and_Design_for_Mechanical_Measure.html?id=KbdYBQAAQBAJ&redir_esc=y.
23. Teussingka T, Simo-Tagne M, Njankouo JM, et al. (2023) An experimental and theoretical analysis of the dynamic response of solar drying in natural convection under rainy month of Maroua (Cameroon) of three tropical wood species. *Wood Material Sci Eng* 1–21. https://doi.org/10.1080/17480272.2023.2178030
24. Wheeler AJ, Ganji AR, Krishnan VV, et al. (2010) Introduction to engineering experimentation. *London, UK: Pearson, Prentice Hall, 2010.* Available from: https://books.google.iq/books/about/Introduction_to_Engineering_Experimentat.html?id=crppr4QT068C&redir_esc=y.
25. Yassen TA, Al-Kayiem HH (2016) Experimental investigation and evaluation of hybrid solar/thermal dryer combined with supplementary recovery dryer. *Sol Energy* 134: 284–293. https://doi.org/10.1016/j.solener.2016.05.011

Appendix A

A.1. Measured parameters uncertainty analysis

The widely errors sources can be divided into three groups as: the error from calibration, data collection, and data reduction. There are many sources of the error's elements for any group. The provided the manufacturer of measurement devices or instruments and various information systems as in the list of specifications such as, linearity, accuracy, drifts, hysteresis and repeatability. The bias error (β) and precision limit (P) have been found using the root-sum-squares (RSS) method for the independent parameters such as temperature, dimensions, etc.:
The bias error (β) can be calculated as [22,23]:

$$\beta = \pm[(\frac{1}{2}Resolution)^2 + (\,Accuracy)^2\,]^2 \tag{7}$$

The average value the measuring scale as:

$$\bar{x} = \frac{1}{n}\sum_{i=1}^{n} x_i \tag{8}$$

The standard deviations (σ_x) of the distributed data of the sample can be calculated as:

$$\sigma_x = [\frac{1}{n-1}\sum_{i=1}^{n}(x_i - \bar{x})^2\ ]^{\ 1/2} \tag{9}$$

The mean standard deviations ($\sigma_{\bar{x}}$) for the sample was derived as follows:

$$\sigma_{\bar{x}} = \frac{\sigma_x}{\sqrt{n}} \tag{10}$$

In order to perform the student–t distribution at 95% confidence interval with the (N-1) freedom degrees, the overall precision error limits can be written as follows:

$$P_x = t(N-1), 95\% \times \sigma_{\bar{x}} \tag{11}$$

The 95% of the confidence uncertainty (U_x) can be evaluated from:

$$U_x = \pm[\beta^2 + P_x^2\,]^{1/2} \tag{12}$$

The percentage relative uncertainty can be predicted as follows:

$$\frac{U_x}{x}\% = \pm(\frac{U_x}{x}) \times 100 \tag{13}$$

For the equations above from (A2) to (A7) the x was an independent parameter. The solar radiation (I) uncertainty value was within the range of ±7.10% and for the ambient temperature (T_a) was ±3.51%. Furthermore, the uncertainty values of the inlet water temperature (T_{in}), outlet water temperature (T_{out}), and the stored water temperature at the time of final withdrawal (T_{wf}) were ±3.55%, ±3.66%, ±4.29%, respectively. Table S1 illustrated the calculated uncertainty for the parameters mention in the current paragraph.

Table S1. The uncertainty of the measured parameters.

	β	$\bar{x}$	(dev.) σ_x	(dev.)$\sigma_{\bar{x}}$	P_x	U_x	$\%\frac{U_x}{x}$
I (W/m^2)	±0.5	1240.5	55.5	27.7	88.141	88.142	±7.10
T_a (℃)	±0.05	16.35	0.36	0.18	0.572	0.574	±3.51
T_{in} (℃)	±0.05	20.62	0.47	0.23	0.731	0.733	±3.55
T_{out} (℃)	±0.05	73.75	1.7	0.85	2.7047	2.705	±3.66
T_{wf} (℃)	±0.05	80	2.16	1.08	3.436	3.436	±4.29

A.2. Thermal efficiency uncertainty analysis

In a general case, consider R as a function of n measured variables (x_1, x_2, …..x_n) as follows [24,25]:

$$R = f(x_1, x_2, \ldots\ldots x_n) \tag{14}$$

A small variance, δR in R due to the small changes δxi's in the xi's through the differential equation as:

$$\delta R = \delta x_1 \frac{\partial R}{\partial x_1} + \delta x_2 \frac{\partial R}{\partial x_2} + \cdots + \delta x_n \frac{\partial R}{\partial x_n} = \sum_{i=1}^{n} \delta x_i \frac{\partial R}{\partial x_i} \tag{15}$$

For a mathematical form, this became as:

$$w_R = \sum_{i=1}^{n} w_{x_i} \frac{\partial R}{\partial x_i} \tag{16}$$

In this experimental study the thermal efficiency function to different measured parameters such as:

$$\eta_{wl} = f(\dot{m}, T_{wf}, T_{out}, T_{in}, I) \tag{17}$$

Finally, after calculations, the uncertainty of the overall thermal efficiency of the ICS-SWH was equal to 3.3%.